*J. Fluid Mech.* (1968), *vol.* 34, *part* 1, *pp.* 113–143
*Printed in Great Britain*



# Pressure-forcing of tightly fitting pellets along fluid-filled elastic tubes

By M. J. LIGHTHILL
Imperial College, London

(Received 25 January 1968)

Some insight into the behaviour of tightly fitting solid pellets, which may be deformable, and are being forced by a pressure difference to move slowly along a distensible tube filled with viscous fluid, is sought by theoretical study of a simple axisymmetric model (§2). In this, the pellet's clearance in the tube is taken to be a small fraction of the tube radius; the fraction may, at a pressure characteristic of that ahead of the pellet, be either positive or negative. Even if it is positive, the tube may still be distended (or the pellet compressed, or both) as the pellet passes, because the thickness of lubricating film generated may exceed the clearance. Naturally, still greater elastic deformation can occur in the case of negative clearance.

Highly simplified elastic properties are assumed; with an eye on tubes occurring in physiological systems (with Poisson's ratio close to 0·5), the local distension of the tube is taken to vary linearly with the local excess pressure; as a still cruder approximation, a similar relation for local reduction of pellet radius is assumed. A parabolic approximation to the pellet's undistorted meridian section, in the region where the lubricating film is thin, is also assumed, leading to a simple relation between pressure and local film thickness which is used, together with Reynolds's lubrication equation, to evaluate both. An arbitrary constant, the rate of leakback of fluid past the pellet, is determined by the condition that the pressure difference forcing the pellet must just balance the skin-frictional resistance to its motion.

The problem is non-dimensionalized (§3) and reduced to that of finding a particular solution of a differential equation containing a certain parameter $L$. In addition to numerical solutions for particular values of $L$ (§6), perturbation solutions for both small and large $L$ are obtained (§§4 and 5), to give mathematical and physical insight; the perturbation for large $L$ (corresponding to negative clearance) is highly singular, requiring the matching of approximate solutions different in each of six different layers.

A striking feature of the solutions is a necking of the gap between pellet and tube behind the pellet. This is so pronounced in the case of negative clearance (figure 2) that it might give the false impression that the pellet was being propelled by peristaltic contraction of the tube instead of by fluid pressure gradient. The physical reason for this is elucidated (§6).

In the case of positive clearance, rather small pressure differences suffice, on this theory, to propel the pellet, because different parts of the lubricating layer

act on it with frictional resistances of different signs, which almost cancel out. By contrast, for negative clearance, the resistance becomes a large multiple of that found in a purely fluid-filled tube of length and mean velocity equal to that of the pellet. This multiple increases, and the film thickness correspondingly decreases (figure 7), as the pellet velocity decreases.

One physiological system on which the model may throw some light is the narrow capillary with red blood cells being squeezed through it in single file, lubricated by plasma (§§1 and 8). At the higher flow speeds, around 0·1 mm/s, the lubricating film, predicted to be about 0·2 $\mu$m thick, appears likely to play a significant role in mass transfer to and from the tissue spaces. At much lower speeds, predicted film thicknesses are so small that any of a number of mechanisms, including loss of fluid through the porous capillary wall due to the local excess pressure in the layer, might cause movement to 'seize up' altogether.

## 1. Introduction

There are many biological systems in which relatively tightly fitting pellets of solid matter are forced along distensible tubes. In some of them, such as the gastro-intestinal system, the motion may be generated by waves of peristaltic muscular contraction passing along the tube. In others, with which this paper is concerned, the motion is generated passively by pressure differences in a fluid with which (in addition to the pellets) the tube is filled.

An example of this on a microscopic scale is the movement of blood through very narrow capillaries. The human red blood cell in the unstressed state is a biconcave disk of diameter about 8 $\mu$m, but under stress is rather easily deformed (Prothero & Burton 1962*b*; Rand & Burton 1964). The narrowest capillaries, which are thought by contrast (Fung 1966) to be much less compliant, have an internal diameter of 5 to 10 $\mu$m. The red cells typically occupy 45 % of the blood volume, most of the remainder being occupied by a viscous fluid, the blood plasma.

Although whole blood possesses anomalous flow properties, such as might be expected of a concentrated suspension of solid matter in fluid, evidence is accumulating that the blood plasma is a Newtonian viscous fluid to a close approximation. In particular, Gabe & Zatz (1968) showed that experiments once believed to suggest a contrary conclusion had been misleading owing to surface effects. When these were eliminated, the amplitude and phase of particle movements in oscillatory azimuthal flow between concentric cylinders agreed very accurately with calculations for a Newtonian fluid.

These considerations indicate that blood flow through a narrow capillary must involve the passage of individual red cells in single file along it, each separated from the one in front by what Prothero & Burton (1961, 1962*a*) described as a 'bolus' of viscous fluid. This motion in single file can, in appropriate tissue, be observed under a microscope. It must be expected that the cells are deformed elastically to enable them to pass through the tube, which may also itself suffer some small elastic distension.

The purpose of this paper is to get some qualitative and quantitative insight into the special problems of flow in tubes under these conditions, including con-

sideration of the lubricating film of plasma which must be present between each red cell and the tube wall. This film is potentially important in regard both to mass transfer and to hydraulic resistance, as well as to the relative residence times of red cells and plasma in the capillary network.

Mass transfer of dissolved gases between pulmonary capillaries and alveoli, or between systemic capillaries and tissue spaces, is evidently of great importance. Forster (1963) has emphasized, moreover, that the pulmonary membrane's impedance to transfer of dissolved gases is not so great that impedance of pathways within the capillaries can be neglected (see p. 842, where the 'diffusing capacities' of which he speaks are effectively reciprocals of impedances); in particular, he argues that gas 'tensions' (what a physical chemist would call their 'fugacities', and which coincide in dilute solution with their vapour pressures) cannot be supposed simultaneously to take approximately equal values at all points in the capillary plasma and at red-cell surfaces.

Prothero & Burton (1961) pointed out that the bolus of viscous plasma between two red cells must perform, relative to their motion, a toroidal circulation, forward on the tube axis and backward near the walls; and that this motion must play a role in limiting differences in gas tensions, and, generally, impedance to mass transfer within the capillaries. It can, however, be argued (see below) that motions within the lubricating film may play an even greater role in these respects.

The relative significance of convection, as compared with simple diffusion, depends on the value of a Péclet number $Ud/D$, where $U$ is a mean velocity, $d$ the tube diameter and $D$ the diffusion coefficient. This takes values of order 1 when the orders of magnitude of $U$, $d$ and $D$ are 0·1 mm/s, 10 $\mu$m and $10^{-3}$ mm$^2$/s. Prothero & Burton showed in model experiments using heat transfer in water that transfer is considerably augmented by convection at such values of the Péclet number, although inertial effects may have caused some slight enhancement of the toroidal vortical motion in their experiments as compared with microcirculatory flows where the Reynolds number $\rho Ud/\mu$ is less than $10^{-2}$.

Within the systemic capillaries, transfer of complex molecules including proteins may be influenced to a greater extent still by convective motions, owing to the very considerably lower values of diffusion coefficients which they in general possess. Landis & Pappenheimer (1963) refer to the distribution and rate of flow of capillary blood as essential factors in such diffusion. Shearing motions in a thin lubricating film may be rather effective in this respect.

Some mass transfer into the tissue spaces is viewed as occurring not diffusively but convectively, the walls of the systemic capillaries being to some extent permeable to liquid through pores of diameter around 8 nm (Guyton 1966). At the upstream end of a narrow capillary, some fluid (although less than 1 % of the total flow) may be forced out by the relatively high pressure,† and the same fluid, after movement through the tissue spaces and some chemical alterations, may be sucked in later by the relatively low pressure in the downstream end of the tube (with the exception of a small proportion returning through the lymphatic

† Large enough to overcome a combination of the mechanical pressure external to the capillary and the opposing difference of osmotic pressure of plasma proteins too large to penetrate pores.

circulation). But the present study reminds us, additionally, that elevated pressures where an individual red cell is squeezed against the capillary wall may possibly do some more local forcing out of fluid, which can return through unstressed parts of the tube wall.

A hydrodynamicist might suppose the hydraulic resistance of the narrowest capillaries to be a factor of great importance in determining overall resistance of the vascular bed, but this is not so, because their extremely low individual conductances are enormously multiplied, in effect, by there being such large numbers of them in parallel. The branchings in the cardiovascular system succeed in economically distributing the blood to a very large mass-transfer area while normally avoiding flow separation and regions of 'dead fluid', which might in fact be deleterious for various reasons (see, for example, Roach (1963, 1964) for evidence of damage to arterial walls by rapid turbulent pressure fluctuations resulting from flow separation). Because in the arteries the velocity drops at each branch by not more than 20 %, separation is normally avoided; the pressure gradients predicted by Poiseuille's law increase under these conditions at each branching. In the arterioles and capillaries, however, Reynolds numbers are of the order of 1, or considerably less, and separation is accordingly most unlikely to occur, even with the much greater velocity reductions which (whether or not for this reason) occur at typical arteriolar and capillary branchings. Now, at a branching, pressure gradients predicted by Poiseuille's law decrease for such velocity reductions of more than 30% (McDonald 1960). These considerations are rightly regarded as strong evidence that the larger arterioles, with diameters of the order of 0·1 mm, give the biggest contribution to the resistance of the vascular bed; it is, furthermore, changes in their diameters (by action of vasomotor muscles) which mainly control the flow, and alter the rates of perfusion of different parts of the capillary circulation.

Nevertheless, capillary resistance could not necessarily be neglected if for any reason it was much greater than the value indicated by Poiseuille's law. Prothero & Burton (1962*a*) estimated from their model experiments the pressure drop in the 'bolus' of moving plasma between two red cells and deduced a contribution to overall capillary resistance less than that given by Poiseuille's law, mainly because plasma with red cells separated out has a viscosity considerably lower than typical values measured for whole blood.

The present studies indicate, however, that the additional contribution to capillary resistance from the pressure difference needed to push a red cell against the viscous drag associated with the lubricating film can, under some conditions, be much greater than that given by Poiseuille's law. Especially when velocities of motion are low, film thicknesses are predicted to be very small and resistance correspondingly high. The possibility is suggested, therefore, as at least worth investigation, that throttling the arterioles may be particularly effective because, at the lower flow speeds that result, there is also a substantial increase in capillary resistance.

Hydrodynamic lubrication is often observed to break down when the film thickness demanded by the dynamics is too small. Opposing roughness elements on the sliding surfaces may then engage so that the motion 'seizes up' altogether. In the present case, the slow forcing of fluid through the tube wall in regions of

elevated pressure might produce a further reduction of film thickness and facilitate this seizing-up process.

Liquid films are essential, in fact, to permit free sliding (which is impossible even to skaters on ice too cold to allow such a film to form under the pressure of their skates). A plasma film will form to lubricate the red cell's passage if this is dynamically possible. The red cell and capillary wall are covered with lipid membranes, but their surfaces are relatively hydrophilic; thus Zubairov, Repeikov & Timerbaev (1963) showed that plasma 'wets' the capillary wall, having an angle of contact around 20°. Certainly, such hydrophilic fatty surfaces as soaps lose their slipperiness in the absence of a water film.

It is well known that arterioles can be throttled to such an extent that capillary motion stops altogether. Under conditions of high vasomotor tone this may be due to throttling actually stopping motion through the relatively easily constricted arterioles. The present work suggests that another mechanism may under other conditions operate: namely that when flow speeds are sufficiently reduced hydrodynamical lubrication in the capillaries gets replaced by solid friction, which can support differences of pressure without the red cells moving at all.

The 'residence times' of red cells in the capillary network are on the average much shorter than those of plasma; indeed, the statistical distributions of residence times of red cells and plasma hardly seem to overlap, indicating that the plasma close to an arterial red cell is, when the cell reaches the veins, all left far behind it. The leakback here studied is an important mechanism for giving plasma a lower mean velocity than red cells in capillaries, while the process known as 'axial concentration' is important in larger vessels such as arterioles. The haematocrit (volume concentration of red cells in the blood) is somewhat lower in the capillary network than in arteries or veins because red-cell residence times are less than those of plasma.† Furthermore, leakback through relatively thin films is important as a mass-transfer mechanism, causing all fluid that is near the capillary wall to be brought rather frequently into close proximity to red cells.

In what follows, some preliminary insight into the problem of motion in narrow capillaries is sought, for the reasons indicated above, by studying an exceedingly simplified dynamical model. In this, loss of fluid through the walls is neglected; the whole motion is taken to be symmetrical about the axis of the tube, and the geometrical and elastic properties of the red cell and the capillary wall are drastically approximated.

In contrast to these simplifications, considered defensible in a preliminary study, certain features of the problem have been regarded as necessary to be retained if any insight was to be got at all. First, a pressure distribution with a local peak must be elastically demanded as the pellet (a word used henceforth in preference to 'red cell', in recognition of the high degree of simplification inherent in the model) moves along the tube. Secondly, the thickness of that gap must be such that viscous forces on the fluid within it balance the gradient of the pressure distribution. Thirdly, the pressure forces and the viscous forces, which constitute the sole external forces on the pellet, must be in equilibrium.

† But a further reduction is thought (Pappenheimer & Kinter 1956) to occur in some organs, such as the kidney, by 'skimming' of plasma from near the walls of arterioles into the fine capillary network, which is by-passed by the remaining cell-rich fluid.

The second condition implies the use of the theory of hydrodynamic lubrication, as developed by Reynolds and his successors, to explain the behaviour of devices such as thrust bearings, in which a large normal force is transmitted between surfaces in rapid relative tangential motion separated by a thin film of viscous fluid. In recent years, certain workers (see, for example, Dowson & Higginson 1960) have extended this theory to the case of thrusts so high that the resulting elastic deformation of the metal surfaces makes a significant alteration to the distribution of film thickness; thus they have included also the first condition. Other workers, for example Christopherson & Dowson (1959), although ignoring elastic effects, have combined the second and third conditions when they considered the motion of nearly tightly fitting rigid pellets in rigid tubes filled entirely with fluid. To the author's knowledge, however, the present investigation is the first in which all three of the above conditions are satisfied.

Furthermore, the main developments in 'elastohydrodynamic' lubrication theory (satisfying the first and second conditions) have notably used the fact that lubricating oils show a great increase in viscosity as pressure rises up to the levels considered. Grubin (1949) inferred an approximation from this which has been widely used and, on the whole, has stood up well to subsequent examination (Dowson & Higginson 1960); a central region, in which film thickness is essentially constant, is on this approximation surrounded by an outer region in which pressures are too low to produce significant deformations.

In physiological problems, of course, pressure changes are insufficient to change fluid viscosity, and such a drastic approximation is then inadequate. Under certain conditions, however, an analogous approximation is possible (§5) involving a central region where there is only a slow variation in film thickness.

In formulating the axisymmetrical problem studied in this paper, and stated in detail in §2, effort has been made to give it generality and potential application to other physiological systems. In some of these the tube might be much more compliant than the pellets (although in the capillaries the reverse is held to be the case). The theory, on the simple elastic assumptions here used, indicates however that the distributions of pressure and film thickness depend only on the sum of the compliances of pellet and tube.

In relation to general problems of slow forcing of pellets along distensible tubes by pressure differences, an interesting conclusion of the work is that there is a 'necking' of the gap behind the pellet, but not in front (see figure 2). This might make the tube look as if it were propelling the pellet by peristaltic contraction, even though the forcing is actually carried out entirely by fluid pressure difference. Mere appearance, then (in contrast to clear evidence of muscles receiving signals to contract), cannot distinguish between hydrodynamically lubricated pressure-forcing and peristaltic propulsion.†

To understand the necking physically, we must recognize that pressure gradient is controlled by the thickness $h$ of the lubricating film in two ways (§6). In

† In other cases, when the pellet is much more compliant than the tube (as for motion in capillaries), the lubricating film is still constricted at the rear, where suction makes the pellet wider than at its point of unconstrained maximum width, just as Bretherton (1961) proved to happen for a bubble moving through a fluid-filled tube.

the absence of leakback of fluid relative to the advancing pellet, a negative pressure gradient proportional to $\mu U/h^2$ (as indicated by dimensional considerations, in terms of fluid viscosity $\mu$ and pellet velocity $U$) would result. Leakback at a rate equal to $Q$ times the tube circumference generates in addition a positive pressure gradient proportional to $\mu Q/h^3$, needed to overcome viscous resistance to leakback. The sum of the two contributions can take any positive value (for some appropriately small value of $h$), but possesses a negative minimum (at some larger value).

Behind the point $P$ of maximum pellet diameter (close to which a pressure maximum is expected) a positive pressure gradient, increasing with distance from $P$, should appear, as long as film thickness remains small, and hydrodynamically this requires $h$ to decrease slightly. No limit to the positive pressure gradient so attainable exists; hence adjustment to the actual level of upstream pressure can be made only by an expansion in film thickness so sudden that pressures actually rise again, a local negative minimum in the pressure gradient being reached momentarily in the process. By contrast, ahead of $P$, no such 'necking' is anticipated, because the pressure gradient, which the geometry requires to be negative, can intensify till it reaches its negative minimum and then slowly rise again to zero while the film thickness increases quite gradually.

These considerations indicate also, what the detailed analysis confirms, that, as $U$ decreases, the film thickness $h$ required to produce the necessary pressure distributions should ultimately vary as $\sqrt{U}$; it follows that the pressure difference, needed to force the pellet against viscous resistances of order $\mu U/h$, also varies ultimately as $\sqrt{U}$. In relatively fast flow conditions, while film thickness is still large, leakback may be rather successful in bringing fluid from close to the capillary wall rapidly into close proximity to the red-cell surface, and so promoting mass transfer. Under slow flow conditions on the other hand, the film may become too thin for hydrodynamical lubrication to be maintained at all.

The conclusions for the model are set out in terms of the mutual dependence of five non-dimensional parameters: a velocity parameter $A$, a clearance parameter $B$ (referring to the clearance, whether positive or negative, of the pellet in the tube if both had the shapes which they would take up at a pressure equal to that of the fluid ahead of the pellet), a typical-film-thickness parameter $C$ and two alternative non-dimensional forms ($D$ and $E$) of the pressure difference forcing the pellet. Various graphical representations of how any two of these parameters determine the other three are given (figures 6–8).

The calculations, although on drastically simplified assumptions, are thought to have some crude quantitative relevance to the squashed red cell in a capillary, even though its geometry is not axisymmetric and its elastic properties are much more complicated than have been assumed. Where the tube wall most pinches the cell, local pressure maxima must be found, and the lubricating film must so adjust itself that the pressure distribution in it, which includes these maxima, is balanced by viscous forces; also the viscous resistance associated with this film must be balanced by the pressure difference forcing the cell along. These considerations seem to indicate that the model may be a first approximation with some indicative value. However, if the problem should prove to have physio-

logical significance, it may well become desirable to make more refined studies later, taking more accurate geometrical or elastic properties, or wall permeability, into account.†

After the work was completed, the author's attention was drawn to a paper by Whitmore (1967), in which the importance of thin films surrounding red cells in capillaries is valuably emphasized. Whitmore's analysis is applicable mainly to the not-so-narrow capillaries for which effects of elastic forces on film thickness (which he does not attempt to estimate) would be negligible. For these, he sees leakback as increasing with tube diameter to a maximum and then decreasing again as tube diameter reaches two or three times the red-cell diameter. The vessels for which leakback was greatest would be those in which the red-cell concentration was a minimum. Furthermore, statistical variations in leakback, caused by variations in red-cell geometry, are suggested as a possible cause for the 'bunching' of red cells that is often observed.

This introduction has suggested application of the analysis only to biological systems, but it should finally be noted that engineering application is not excluded; for example, to the cleaning of fluid out of long pipelines by passing rubber pellets along them.

## 2. Mathematical statement of the lubrication problem

The simplifications made, to render the lubrication problem discussed in § 1 fairly tractable while retaining its essential features, are, in detail, as follows.

Geometrically, the tube and pellet are supposed axisymmetrical. The maximum diameter of the pellet is supposed greater or less than that of the tube by only a small fraction, at any rate under a pressure characteristic of, say, the fluid into which the pellet moves. In other words, there is reasonable approximation (either on one side or the other) to a good fit. It is, as we shall see, only parts of the surface at a distance from the axis nearly equal to the tube radius whose shape significantly influences the lubrication problem. In many cases, these limited parts will be characterized geometrically to good enough approximation by the curvature $\kappa$ of the pellet's meridian section at its point of maximum diameter. We may therefore simplify the problem, while remaining reasonably realistic, by taking that meridian section, at a certain reference pressure $p_0$ which will be defined later, to have the equation

$$r = r_0 - \tfrac{1}{2}\kappa x^2, \tag{1}$$

where $x$ is measured axially downstream from the point where the pellet cross-section has its maximum radius $r_0$.

The elastic properties of the tube are also taken as simple as possible without being ignored altogether. The inner diameter at any one point is taken to increase linearly with the local pressure, but not to depend on the pressure at any other point. Implicit in this is the assumption that the tube is not under longitudinal tension (which would add a term proportional to the curvature of the meridian

† *Note added in proof.* Work on all these lines by J. M. Fitz-Gerald has now reached an advanced stage.

section). Furthermore, the internal pressure itself is assumed not to generate axial tensions; this assumption is at least reasonable for tube materials with Poisson's ratio close to $\frac{1}{2}$, like those occurring in most biological systems. It is convenient to write the linear relation between local internal radius of tube wall $r$ and local pressure $p$ as

$$r = r_0 + \alpha(p - p_0) \tag{2}$$

so that the reference pressure $p_0$ (which may be positive or negative relative to atmospheric pressure) is defined by (1) and (2) as that for which elastic deformation causes the pellet to fit exactly within the tube. This means that pressure distributions with $p > p_0$ everywhere correspond to pellets whose maximum diameter is less than the minimum internal diameter of the tube, but distributions including regions where $p < p_0$ correspond to tubes whose diameter is in places less than the pellet's maximum diameter.

Cases where the deformability of the pellets may be ignored could, without doubt, be of some interest. A more general case, in which elastic properties of the pellet are not completely ignored, but are highly simplified, is one in which difference in the local pressure from the reference pressure $p_0$ produces a proportionate local constriction of the local pellet radius below the value (1):

$$r = r_0 - \tfrac{1}{2}\kappa x^2 - \beta(p - p_0). \tag{3}$$

(Where pellets of complex internal structure are involved, such a dependence is thought to be the only reasonable relatively simple assumption that can be made.) We shall see that the radial compliances $\alpha$ and $\beta$, of tube and pellet respectively, are not separately significant, but appear only in the linear combination $\alpha + \beta$.

In fact, the thickness $h$ of the lubricating film between the pellet and the inner tube wall must be given as the difference between the two radii (2) and (3), namely as

$$h = (\alpha + \beta)(p - p_0) + \tfrac{1}{2}\kappa x^2. \tag{4}$$

Since this thickness must be positive, we see that the point $x = 0$ of maximum pellet diameter $p - p_0$ must be positive, although other regions may exist (as has already been noted) where $p < p_0$.

When a pellet is being forced along the tube by fluid pressure difference at a velocity $U$, we may conveniently analyse the dynamics of the lubricating film in a frame of reference which itself moves with the pellet at velocity $U$. There is then a steady flow in which the axial velocity takes the value zero at the pellet and the value $(-U)$ at the tube wall. To obtain axial velocities relative to the tube, it would of course merely be necessary to add $U$.

The film will now be analysed on the usual assumptions of hydrodynamic lubrication theory. In particular, the Reynolds number based on film thickness is assumed small enough so that the inertial terms can be neglected in the equations of motion. The other approximations are those of boundary-layer theory; in particular, the pressure $p$ is taken to depend on the axial co-ordinate $x$ alone and not to vary across the layer, and the thickness $h$ is taken to be much smaller than the reference radius $r_0$ of pellet or tube in all parts of the flow where the pressure $p$ is varying significantly owing to hydrodynamic lubrication effects.

As usual in theories of boundary-layer type, we use a special co-ordinate $y$ to denote distance across the layer; in this case, radial distance measured from $y = 0$ at the surface of the pellet (so that $y$ is in fact the difference between $r$ and the right-hand side of (3)). The axial momentum equation (boundary-layer equation without inertial terms) takes the form

$$\frac{dp}{dx} = \mu \frac{\partial^2 u}{\partial y^2}, \tag{5}$$

where the right-hand side is the usual boundary-layer approximation to the viscous terms, so that, for example, a term like $(\mu/r)\,\partial u/\partial y$ has been neglected because typical values of $h$, where the pressure is varying significantly, are small compared with typical values of $r$.

Equation (5) must be solved subject to boundary conditions

$$u = 0 \ \ (y = 0), \quad u = -U \ \ (y = h), \tag{6}$$

as has already been discussed, and to an equation of continuity

$$\int_0^h u\,dy = -Q, \tag{7}$$

where $Q$ is independent of $x$ and $2\pi r_0 Q$ represents a rate of leakback of fluid past the pellet. To obtain (7), the equation of continuity in the approximate form

$$\partial u/\partial x + \partial v/\partial y = 0, \tag{8}$$

which neglects such relatively smaller terms as $v/r$, must be integrated from $y = 0$ to $y = h$, so as to eliminate $v$.

The distribution of $u$ across the layer given by (5) must be quadratic, since $\partial^2 u/\partial y^2$ is independent of $y$, and equations (6) and (7) determine it uniquely as

$$u = U\left[2\frac{y}{h} - 3\left(\frac{y}{h}\right)^2\right] - \frac{6Q}{h}\left[\frac{y}{h} - \left(\frac{y}{h}\right)^2\right]. \tag{9}$$

Substitution in (5) then gives

$$\frac{dp}{dx} = -\frac{6\mu U}{h^2} + \frac{12\mu Q}{h^3}, \tag{10}$$

a second relation between the pressure $p$ and the film thickness $h$ (both being functions of $x$), which together with the relation (4) constitutes a differential equation for either quantity. The increasing inaccuracy of the assumptions leading to equation (10) as $h$ becomes large (far from the point $x = 0$ of maximum pellet diameter) is evidently unimportant because the pressure gradient soon becomes negligibly small in this region compared with its values where the film is thin.

Thus, the differential equation specified by (4) and (10) has solutions with definite limits $p(\infty)$ and $p(-\infty)$ as $x$ becomes large. Although mathematically these are limits as $x \to \infty$ or $x \to -\infty$, they represent in practice values of the pressure such as would be found immediately ahead of and behind the region where the lubricating film is thin.

Specifying the downstream pressure $p(\infty)$ would essentially determine the positive or negative clearance $(\alpha+\beta)[p(\infty)-p_0]$ of the pellet in the tube at that downstream pressure. Also it would specify uniquely a solution of equation (10), and so determine the pressure difference $p(-\infty)-p(\infty)$ required to push the pellet against viscous resistance at the assumed velocity $U$. However, the answer obtained would depend still on one unknown constant $Q$, appearing in (7), (9) and (10), whose value we wish to calculate in its own right as well as a means of evaluating the resistance.

Fortunately, one relationship exists which has still not been used and is suitable for determining the unknown constant $Q$. This states that the axial forces on the pellet are in equilibrium, so permitting it to proceed along the tube at constant velocity $U$. The skin-friction $\tau$ (viscous stress resisting the motion of the pellet) is given by (9) as

$$\tau = -\mu\left(\frac{\partial u}{\partial y}\right)_{y=0} = -\frac{2\mu U}{h}+\frac{6\mu Q}{h^2}, \tag{11}$$

while the total resistance, integrated over the area of the pellet where $h$ is small compared with the reference radius $r_0$, is

$$2\pi r_0\int_{-\infty}^{\infty}\tau\,dx. \tag{12}$$

Balancing this resistance force on the pellet is the axial force due to the pressure difference $p(-\infty)-p(\infty)$ acting over a cross-sectional area that may be approximated as $\pi r_0^2$. Hence, to this approximation,

$$\pi r_0^2[p(-\infty)-p(\infty)] = 2\pi r_0\int_{-\infty}^{\infty}\left(-\frac{2\mu U}{h}+\frac{6\mu Q}{h^2}\right)dx. \tag{13}$$

We shall see that the range of solutions of the differential equation (10) that are physically relevant is considerably restricted by (13). This is because, for both sides to have the same (positive) sign, the solution must be such that, in some average sense, $dp/dx < 0$ but $\tau > 0$. Equations (10) and (11) show this to mean that the layer must be dominated by a region with

$$2Q/U < h < 3Q/U, \tag{14}$$

even though far larger values of $h$ must be present for the larger $|x|$. It is this condition that is satisfied for only a rather restricted band of solutions of the differential equation.

## 3. Reduction to non-dimensional form

In scaling the variables so as to reduce the problem defined in §2 to non-dimensional form, we take into account the expectation just inferred, that $2Q/U$ will be a good measure of typical film thickness. This leads us to non-dimensional forms

$$H = \frac{h}{2Q/U}, \quad P = \frac{(\alpha+\beta)(p-p_0)}{2Q/U}, \quad X = \left(\frac{\kappa}{2Q/U}\right)^{\frac{1}{2}}x, \tag{15}$$

where the pressure is scaled in terms of that required to increase the film thickness (4) by one standard amount $2Q/U$, and axial distance in terms of that required to increase the film thickness by half that standard amount.

Equations (10) and (4) then become

$$dP/dX = L(H^{-3} - H^{-2}), \quad H = P + \tfrac{1}{2}X^2, \tag{16}$$

where the non-dimensional constant $L$, whose value, as we shall see, determines the character of the solution, is given as

$$L = \frac{6\mu U(\alpha+\beta)}{(2Q/U)^{\frac{5}{2}}\kappa^{\frac{1}{2}}}. \tag{17}$$

The subsidiary condition (13) can then be regarded as determining the non-dimensional quantity

$$C = 2Q/Ur_0, \tag{18}$$

which can be interpreted as a ratio of a typical film thickness $2Q/U$ to the reference radius $r_0$. The assumptions of § 2 show that we are interested in solutions with $C$ small compared with 1. A more precise interpretation of $C$ derives from the fact that $2\pi r_0 Q$ is the rate of leakback of fluid past the pellets. Comparing this with the flux $\pi r_0^2 U$ of fluid that the pellets' motion would produce in the absence of leakback, we see that $C$ is the fractional reduction in fluid flow due to leakback, or, in other words, the fractional reduction in mean fluid velocity below the pellet velocity $U$. In terms of $C$, equation (13) becomes

$$P(-\infty) - P(\infty) = LC\int_{-\infty}^{\infty} (H^{-2} - \tfrac{2}{3}H^{-1})\,dX. \tag{19}$$

The non-dimensional form of the equations can in principle be solved uniquely if $L$ is given (implying that $U$ and $Q$ are prescribed, but not at this stage $r_0$), together with say $P(\infty)$, which specifies the positive or negative clearance, which the pellet would have in the tube at the downstream value of the pressure, as a fraction of $2Q/U$. The solution then fixes $P(-\infty)$ and so the pressure difference needed to push the pellet at velocity $U$, while equation (19) fixes $C$, that is, the ratio between the alternative length-scales $2Q/U$ and $r_0$.

The interesting phenomenon, that only a narrow band of solutions of the non-dimensional differential equation (16) fulfils the necessary condition that $C$ be small and positive (or in some cases even the condition that the value of $C$ determined from (19) be positive at all), is well brought out by analysis of solutions both in the limit as $L \to 0$ and in the limit as $L \to \infty$, and numerical solution confirms it. The results of analysis for small $L$ and large $L$ and of computer solutions for a range of intermediate $L$ are given in the sections that follow.

## 4. Analysis for small $L$

For small values of the parameter $L$, the differential equation (16) can be solved by a simple perturbation analysis. However, the interesting question, whether any band of solutions exists such that both the left-hand side of equation (19) and the integral on the right-hand side are positive, as is necessary for a

physically meaningful solution, cannot be answered on a first-order perturbation analysis and requires analysis to third order.

If we write, for convenience, $P(\infty) = \frac{1}{2}\alpha^2$, then the zero-order solution of (16) as $L \to 0$ is $P =$ constant $= \frac{1}{2}\alpha^2$. If this solution is substituted on the right-hand side of the differential equation, the first-order solution follows by integration. To this order, we obtain

$$P(-\infty) - P(\infty) = \frac{2\pi L}{\alpha^5}(\alpha^2 - \tfrac{3}{2}), \tag{20}$$

which is positive provided that

$$P(\infty) = \tfrac{1}{2}\alpha^2 > \tfrac{3}{4}, \tag{21}$$

but we also obtain

$$\int_{-\infty}^{\infty} (H^{-2} - \tfrac{2}{3}H^{-1})\,dX = \frac{4\pi}{3\alpha^3}(\tfrac{3}{2} - \alpha^2), \tag{22}$$

which is only positive if

$$P(\infty) < \tfrac{3}{4}. \tag{23}$$

To this order, then, there is no band of solutions for which both quantities are positive, but, because the bands where each is positive are directly contiguous, it remains possible that when analysed to higher order in $L$ they may overlap.

This is found to be the case, in fact, by an analysis to third order, which although completely straightforward is too lengthy to be reproduced here. The condition (21) that $P(-\infty) - P(\infty)$ be positive becomes replaced by

$$P(\infty) > 0{\cdot}75 - 0{\cdot}1313L^2, \tag{24}$$

while the integral (22) is positive provided that

$$P(\infty) < 0{\cdot}75 - 0{\cdot}1169L^2. \tag{25}$$

For these small values of $L$, therefore, there is an exceedingly narrow band of solutions, namely those satisfying (24) and (25), for which the peremptory requirement that equation (19) yield a positive value of $C$ is satisfied. Evidently the value of $C$ so obtained varies from 0 to $+\infty$ as we go from the lower limit (24) to the upper limit (25), and, since we are in fact interested only in *small* positive values of $C$, it is solutions close to the lower limit (24) which alone can concern us.

For these small positive values of $C$, it is an adequate approximation to replace the integral on the right-hand side of equation (19) by its value *at* the lower limit of the permissible band of solutions. This procedure, which will also be found not too inaccurate for large $L$, is really a continuation of the process of approximating for small $C$, that is, small ratio of film thickness to tube radius, which was involved in the derivation of the equations in § 2. The zero-order approximation for small $C$ to equation (19) selects the solution with $P(-\infty) = P(\infty)$. The first-order approximation for small $C$, which we adopt, uses the zero-order solution to evaluate the integral in (19) as what we shall call

$$f(L) = \text{value of } \int_{-\infty}^{\infty} (H^{-2} - \tfrac{2}{3}H^{-1})\,dX \quad \text{for the solution with} \quad P(-\infty) = P(\infty), \tag{26}$$

and takes

$$P(-\infty) - P(\infty) = LCf(L). \tag{27}$$

The actual third-order analysis for small $L$ gives, in fact,

$$f(L) \sim 0{\cdot}0657L^2 \quad \text{as} \quad L \to 0. \tag{28}$$

We shall also define, for all $L$, $b(L)$ as the value of $P(\infty)$ for the solution specified in (26); equation (24) implies that

$$b(L) - 0{\cdot}75 \sim -0{\cdot}1313L^2 \quad \text{as} \quad L \to 0. \tag{29}$$

This shows how the clearance between pellet and tube at a pressure characteristic of that ahead of the pellet, which $b(L)$ gives as a fraction of the typical film thickness $2Q/U$, is positive for all the smaller values of $L$, although we shall see later that it takes negative values when $L > 3{\cdot}2$. The curious reader might suppose that the coefficients appearing in (28) and (29) are in the exact ratio 2, but this is not so; the former is $2^{\frac{7}{2}} . 3^{-\frac{1}{2}} . 7\pi$ whereas the latter is the rational number 319/2430.

Numerical evaluation of $f(L)$ and $b(L)$ will, in fact, show us that this perturbation analysis for small $L$ leading to (28) and (29) gives reasonable results for $L \leqslant 1$.

## 5. Analysis for large $L$

Complementary to the perturbation analysis for small $L$ just presented is an analysis of the differential equation (16) in the limit as $L \to \infty$. Analysis for large $L$ is important especially because the cases when the clearance between pellet and tube would be negative if both were at the downstream value of the pressure are found to fall into this range. Even though particular numerical solutions of (16) have been computed, an analysis for large $L$ is useful for fitting them into a general scheme, and for giving the kind of physical insight into their form that was offered in a preliminary way in § 1. Conversely, numerical solutions for large $L$ (such as $L = 8$) are found in § 6 to give quite a good check on the correctness of the rather complex analysis of this section.

Evidently the study of equation (16) for large $L$ is a singular-perturbation problem. It is, indeed, one to bring joy to the hearts of devotees of the method of matched asymptotic expansions, since to obtain even a first approximate solution for large $L$ involves matching forms of asymptotic solution that are different in each of six separate layers. The fact that the coefficient of $L$ on the right-hand side of the equation possesses a stationary value when $H = \frac{3}{2}$ is in part responsible for the rather unusual complexity of the multi-layer asymptotic solution.

The six layers comprise, first, three extended regions where the approximate form of the solution is very simple indeed; we shall call them a left-hand region (extending to $X = -\infty$), a central region (including $X = 0$) and a right-hand region (extending to $X = +\infty$). Of these, the first two are separated by a narrow region of simple boundary-layer type; but the central and right-hand regions are separated by a more extended interval which is of double-boundary-layer type, in that it needs asymptotic analysis as a combination of two separate matched layers. All the boundary layers are situated in regions where $|X|$ is of order $L$.

The two outermost regions are constant-pressure regions in which the right-hand side of the differential equation (16) is so small that to a high order of approximation

$$P = P(-\infty) \tag{30}$$

in the left-hand region and

$$P = P(\infty) \tag{31}$$

in the right-hand region. The central region is one of slowly varying film thickness, as mentioned already in §1. In this region, in fact, $H$ varies so slowly with $X$ that to a close approximation the left-hand side of the differential equation (16), namely $dP/dX$, can be replaced by $-X$, giving

$$X/L = H^{-2} - H^{-3}. \tag{32}$$

In this region, equation (32) specifies $H$ as a smooth function of $X/L$, which near $X = 0$ behaves closely like $1 + X/L$. Substitution to obtain a more accurate value for $dP/dX$ shows the error in equation (32) for $H$ to be of order $L^{-2}$.

The matching between the left-hand solution (30) and the central solution (32) takes place in a narrow region where $X$ changes so little that to a first approximation the difference $X$ between $dH/dX$ and $dP/dX$ can be taken constant within the region. We are interested in large negative values of $P(-\infty)$, as we shall see, and for these there is only a short transition between values of $X$ so large and negative that $H^{-2}$ on the right-hand side of the differential equation (16) is completely negligible and values of $X$ which make $H$ of order 1 as in (32).

If this transition layer is centred on a point $X = -Y$ then $\frac{1}{2}X^2$ can be approximated as $-\frac{1}{2}Y^2 - YX$ within the layer, and therefore $dP/dX$ replaced by $dH/dX + Y$. Where this layer merges with the left-hand region, governed by (30), we have

$$H = P(-\infty) + \tfrac{1}{2}X^2 \sim P(-\infty) - \tfrac{1}{2}Y^2 - YX. \tag{33}$$

At a general point of the layer (16) becomes

$$dH/dX + Y = L(H^{-3} - H^{-2}). \tag{34}$$

The general solution of (34) takes the form

$$X = -\int \frac{dH}{Y + L(H^{-2} - H^{-3})} + \text{constant}, \tag{35}$$

and the solution satisfying the condition (33) at the left-hand edge of the layer is

$$\begin{aligned} X &= \frac{1}{Y}[P(-\infty) - \tfrac{1}{2}Y^2 - H] + \int_H^\infty \left[\frac{1}{Y + L(H^{-2} - H^{-3})} - \frac{1}{Y}\right] dH \\ &= \frac{1}{Y}\left[P(-\infty) - \tfrac{1}{2}Y^2 - H - \int_H^\infty \frac{L(H-1)\,dH}{YH^3 + L(H-1)}\right]. \end{aligned} \tag{36}$$

Since $Y$ itself, as we shall see at the end of this section, is of order $L$, the thickness of layer within which (36) holds is of order $1/L$.

This layer terminates on the right at the point $H = H_0$ where the denominator $YH^3 + L(H-1)$ in (36) vanishes. Evidently this is the transition to the central region where (32) holds: at the boundary layer, of course, the $X$ which appears in

(32) is replaced by $-Y$. The integral in (36) becomes logarithmically infinite as $H$ approaches $H_0$, so that $H-H_0$ is tending exponentially to zero as $YX$ increases. This confirms that the boundary layer between the left-hand and central regions has thickness of order $1/L$ and merges with exponential rapidity into the central region.

The adequacy of these approximations depends on an appropriate choice o $Y$, as a typical value of $-X$ in the midst of the boundary layer. It is sufficient to take it as the value where $H$ takes the intermediate value 1, and so obtain $Y$ by solving the equation

$$\begin{aligned} \tfrac{1}{2}Y^2+P(-\infty)-1 &= \int_1^\infty \frac{L(H-1)\,dH}{YH^3+L(H-1)} \\ &= \sum_{n=1}^{\infty}(-1)^{n-1}\frac{(2n-2)!\,n!}{(3n-1)!}\left(\frac{L}{Y}\right)^n. \end{aligned} \tag{37}$$

Before leaving the left-hand boundary layer we may note that a solution uniformly valid between it and the left-hand region can be obtained from (36) by replacing $XY+\frac{1}{2}Y^2$ by $-\frac{1}{2}X^2$ again; this solution is

$$\tfrac{1}{2}X^2 = P(-\infty)-H-\int_H^\infty \frac{L(H-1)\,dH}{YH^3+L(H-1)}, \tag{38}$$

which in the limit as the integral tends to zero becomes identical with equation (30).

An interesting feature of the solutions in the left-hand and central regions and intervening boundary layer is that within very wide limits any large negative value may be taken for $P(-\infty)$, and in the left-hand region this determines a solution (30), but, when the solution is continued far enough to the right, we reach a central region where the solution (32) has ceased to show any dependence on $P(-\infty)$. It is merely the position $X=-Y$ where the transition occurs, and to a minor extent the speed of the transition, that depend on $P(-\infty)$. Sooner or later, all these solutions converge into the one curve given by (32), so we may say that, if we are solving from left to right, the differential equation is an exceedingly stable one.

This high degree of stability, at any rate in the region around $H=1$, can be perceived very clearly if we linearize the differential equation (16) about $H=1$ so that it becomes

$$dH/dX+L(H-1)=X. \tag{39}$$

Evidently the different solutions of (39) differ by constant multiples of $\exp(-LX)$, and all converge on to each other as $X$ increases.

There is a more complicated kind of boundary-layer behaviour between the central and right-hand regions. Whereas on the left the central solution (32) could, in principle, be continued up to any negative value of $X/L$, however large, and the particular value at which it breaks off depends on which particular left-hand solution $P=P(-\infty)$ it must match with, the situation on the right is quite different. We are not dealing now with a bundle of solutions, because they have all run together into one. However, that one solution (32) cannot be continued beyond $X/L=\frac{4}{27}$ because $\frac{4}{27}$ is the maximum value that the right-hand

side of equation (32) can take. In the absence of any other criterion to set a limit on the right to the validity of (32), this maximum is found to dominate the transition. Its presence, furthermore, seriously complicates the problem of approximating to equation (16) around $X/L = \frac{4}{27}$, because changes in $L(H^{-2}-H^{-3})$ *around the maximum* cannot easily be so large as to dominate changes in the $(-X)$ component of $dP/dX$.

Accordingly, an adequate approximation to equation (16) near $X/L = \frac{4}{27}$ involves making a quadratic approximation to $H^{-2}-H^{-3}$ around its maximum $H = \frac{3}{2}$, namely

$$H^{-2}-H^{-3} \doteqdot \tfrac{4}{27}-\tfrac{16}{81}(H-\tfrac{3}{2})^2, \tag{40}$$

but not simplifying in any other way. The equation becomes

$$\frac{dH}{dX} = X+L[\tfrac{16}{81}(H-\tfrac{3}{2})^2-\tfrac{4}{27}]. \tag{41}$$

We need the solution of (41) which fits, on the left-hand side of $X/L = \frac{4}{27}$, into equation (32) as modified by the approximation (40) to the form

$$H = \tfrac{3}{2}-\left[\frac{81}{16}\left(\frac{4}{27}-\frac{X}{L}\right)\right]^{\frac{1}{2}}. \tag{42}$$

That solution of the Riccati equation (41) is obtained by standard methods as

$$H = \tfrac{3}{2}+\left(\frac{81}{16L}\right)^{\frac{2}{3}}\chi\left[\left(\frac{16L}{81}\right)^{\frac{1}{3}}\left(\frac{4L}{27}-X\right)\right], \tag{43}$$

where $\chi(z)$ is the logarithmic derivative of the Airy function; thus

$$\chi(z) = \mathrm{Ai}'(z)/\mathrm{Ai}(z) \sim -\sqrt{z} \quad \text{as} \quad z\to+\infty. \tag{44}$$

This solution (43) is reasonable until $X$ approaches near

$$X_1 = \frac{4L}{27}+z_1\left(\frac{81}{16L}\right)^{\frac{1}{3}}, \tag{45}$$

where $z_1 = 2{\cdot}338$ is the smallest positive root of $\mathrm{Ai}(-z) = 0$. As $z\to -z_1$,

$$\chi(z) \sim \frac{1}{z+z_1}, \quad \text{giving} \quad H-\tfrac{3}{2} \sim \frac{81/16L}{X_1-X}. \tag{46}$$

A second boundary layer is now needed to fit the solution (43), which as $X$ approaches near $X_1$ takes the simple form (46), into the still simpler right-hand solution (31).

Fortunately, this second right-hand boundary-layer solution can be worked out sufficiently accurately by the same approximation that led to the left-hand boundary-layer solution (36). We approximate $\frac{1}{2}X^2$, not now near $X = -Y$ but near $X = X_1$, as $X_1X-\frac{1}{2}X_1^2$. Where the layer merges with the right-hand solution (31), we have

$$H = P(\infty)+\tfrac{1}{2}X^2 \sim P(\infty)-\tfrac{1}{2}X_1^2+X_1X. \tag{47}$$

At a general point of the layer

$$dH/dX = X_1+L(H^{-3}-H^{-2}), \tag{48}$$

and the solution of (48) which agrees with (47) as $X - X_1$ increases is

$$X = \frac{1}{X_1}[-P(\infty) + \tfrac{1}{2}X_1^2 + H] + \int_H^\infty \left[\frac{1}{X_1} - \frac{1}{X_1 + L(H^{-3} - H^{-2})}\right] dH$$

$$= \frac{1}{X_1}\left[-P(\infty) + \tfrac{1}{2}X_1^2 + H - \int_H^\infty \frac{L(H-1)\,dH}{X_1 H^3 - L(H-1)}\right]. \tag{49}$$

Since equation (49) represents a bundle of solutions for different values of $P(\infty)$, it seems likely that the process of matching to the behaviour (46) for $X$ just less than $X_1$ will fix the actual value of $P(\infty)$ uniquely. This is found to be the case if near $H = \frac{3}{2}$ we write the integral on the right-hand side of (49) as an integral from $\frac{3}{2}$ to $\infty$, which we call $G$, minus a second integral from $\frac{3}{2}$ to $H$, and in the latter make the approximation (40). This gives

$$X = \frac{1}{X_1}[-P(\infty) + \tfrac{1}{2}X_1^2 + \tfrac{3}{2} - G] + \int_{\frac{3}{2}}^H \frac{dH}{X_1 - \frac{4L}{27} + \frac{16L}{81}(H - \frac{3}{2})^2}$$

$$= \frac{1}{X_1}[-P(\infty) + \tfrac{1}{2}X_1^2 + \tfrac{3}{2} - G] + \frac{1}{\sqrt{z_1}}\left(\frac{81}{16L}\right)^{\frac{1}{3}} \tan^{-1}\left[\frac{H - \frac{3}{2}}{\sqrt{z_1}}\left(\frac{16L}{81}\right)^{\frac{2}{3}}\right]. \tag{50}$$

When the last quantity in square brackets in (50) takes values large compared with 1, the inverse tangent tends to the constant value $\frac{1}{2}\pi$ with a difference proportional to the reciprocal of its argument. This matches with the behaviour (46) precisely provided that the pole $X = X_1$ is equal to the value of (50) with the inverse tangent set equal to $\frac{1}{2}\pi$; in other words, that

$$X_1 = \frac{1}{X_1}[-P(\infty) + \tfrac{1}{2}X_1^2 + \tfrac{3}{2} - G] + \frac{\frac{1}{2}\pi}{\sqrt{z_1}}\left(\frac{81}{16L}\right)^{\frac{1}{3}}. \tag{51}$$

This equation has been reached by matching solutions in a region where $H - \frac{3}{2}$ is relatively small but $X_1 - X$ is also small; fortunately these conditions are compatible for large enough $L$, as equation (46) shows. Hence, finally, for large enough $L$,

$$P(\infty) \doteqdot -\tfrac{1}{2}X_1^2 + \tfrac{3}{2} - G + \frac{\frac{1}{2}\pi}{\sqrt{z_1}}\left(\frac{81}{16L}\right)^{\frac{1}{3}} X_1, \tag{52}$$

where $X_1$ is given by (45) and

$$G = \int_{\frac{3}{2}}^\infty \frac{L(H-1)\,dH}{X_1 H^3 - L(H-1)}. \tag{53}$$

We have inferred that the value of $P(\infty)$ is, to a good approximation for large $L$, independent of the value chosen for $P(-\infty)$. Actually, since only small values of $C$ are of interest, equation (27) forces $P(-\infty)$ to be not greatly different from $P(\infty)$. But, since the value of $P(\infty)$ depends so little on the value of $P(-\infty)$, it is adequate, just as with small $L$ (§4), to concentrate on that solution for which $P(-\infty) = P(\infty)$. The value of $P(\infty)$ for that particular solution was called $b(L)$ in §4, and equation (52) tells us that for large $L$

$$b(L) \doteqdot -\tfrac{1}{2}X_1^2 + \tfrac{3}{2} - G + \frac{\frac{1}{2}\pi}{\sqrt{z_1}}\left(\frac{81}{16L}\right)^{\frac{1}{3}} X_1. \tag{54}$$

There is a somewhat greater, but not by any means critical, dependence of the integral on the right-hand side of (19) upon the value of $P(-\infty)$; for small enough $C$ it can again be approximated sufficiently accurately by $f(L)$, defined in (26). Essentially this is because the contribution to the integral from the central region outweighs all the contributions from the other five layers. The fact that the integrand vanishes at $H = \frac{3}{2}$ reduces the significance of the relatively thick double boundary layer on the right-hand side, whose influence on the value of $b(L)$, by contrast, is as we shall see quite large even for values of $L$ of order 10. The exponential increase in $H$ in the thinner left-hand boundary layer makes its contribution still smaller.

The main contribution to the integral, then, that from the central region where (32) holds, can be written

$$\int_{H_0}^{\frac{3}{2}} (H^{-2} - \tfrac{2}{3}H^{-1}) L(-2H^{-3} + 3H^{-4}) dH = \left(\frac{3}{5H_0^5} - \frac{1}{H_0^4} + \frac{4}{9H_0^3} - \frac{16}{1215}\right) L, \quad (55)$$

where the range $H_0 < H < \frac{3}{2}$ is the range of validity of the central solution and $dX$ has been substituted from equation (32). The coefficient of $L$ in (55) shows some dependence on the value of $P(-\infty)$ through equation (37) defining $Y$, which in turn specifies $H_0$ as the solution of

$$H_0^{-3} - H_0^{-2} = Y/L. \quad (56)$$

In the particular case $P(-\infty) = P(\infty)$ used in (26) to define $f(L)$, we have asymptotically for very large $L$, according to (45) and (51), $X_1 \sim 4L/27$ and

$$P(-\infty) = P(\infty) \sim -\frac{8L^2}{729} = -0{\cdot}0110L^2, \quad (57)$$

so that in turn, by (37), $Y \sim 4L/27$, from which equation (56) gives $H_0 = 0{\cdot}894$ and finally (55) gives

$$f(L) \sim 0{\cdot}094L. \quad (58)$$

If we used this asymptotic equation (58) in combination with equation (27) in the case $C = 0{\cdot}05$, say, we should get, as an approximation to $P(-\infty)$ closer than (57), the result $P(-\infty) \sim -0{\cdot}0063L^2$, and so should obtain $Y \sim 0{\cdot}112L$ and $H_0 = 0{\cdot}914$, whence the integral (55) would come to $0{\cdot}077L$. This value would then lower $P(-\infty)$ a little, and so on; when the process has converged, the true value of the integral (55) comes to $0{\cdot}079L$. We can say, therefore, that for $C = 0{\cdot}05$ the use of $f(L)$ as defined by (26) to determine through (27) the resistance to the pellet's motion overestimates the true resistance by as much as 19 % when $L$ is very large. On the other hand, similar analysis of the results of § 4 indicates that for small $L$ the overestimate is considerably less substantial; furthermore, we shall find in § 7 that practical cases with $C$ as big as $0{\cdot}05$ to which the theory applies correspond to relatively small values of $L$ (not exceeding 5).

The general conclusion of these analyses is that errors are not expected to be too great if a single solution of equation (16) is obtained for each $L$, namely that for $P(-\infty) = P(\infty)$, and if the difference $P(-\infty) - P(\infty)$ is then determined from equation (27). This is a useful simplication, which is used throughout the numerical work described in § 6, and whose validity will be supported by further studies in § 7.

## 6. Numerical analysis for particular values of $L$

The rather complicated nature of the perturbation analyses of §§4 and 5 for small $L$ and large $L$ respectively made it desirable to obtain solutions of (16) numerically for a representative set of values of $L$. For reasons just described, however, only solutions with $P(-\infty) = P(\infty)$ were calculated.

To make the equation suitable for numerical integration on a computer using the Runge–Kutta method, a finite range of integration was obtained by the transformation $X = (\sqrt{2})\tan\theta$. The interval from $\theta = -\frac{1}{2}\pi$ to $\theta = \frac{1}{2}\pi$ was divided into $44L$ equal intervals, this number being chosen in the light of the analyses for small and large $L$ to allow for proper following of the regions where the most rapid variation of $P$ with $X$ was expected; for example, for large $L$, the left-hand boundary layer. Integration was performed in the 'stable' direction (from left to right, see §5) and iteration used to find the solution with $P(-\infty) = P(\infty)$. The grid points were dense enough for the integral $f(L)$ defined by (26) to be determined by application of the trapezium rule; for this purpose the limit of the transformed integrand as $\theta \to \pm\frac{1}{2}\pi$ had to be calculated analytically.

Solutions for $L = 0{\cdot}5, 1, 2, 3, 4, 6, 8$ and 10 were obtained by these means. Some aspects of them are set out graphically in figures 1 to 5. First, the quantity $b(L)$ representing the value of $P(\infty)$, which signifies the clearance of the pellet in the tube at the downstream value of the pressure as a fraction of the typical film thickness $2Q/U$, is plotted as a function of $L$ in figure 1. This plot gives a useful clue to the significance of different values of the parameter $L$, whose own definition (17) is rather complicated. We see that for $L < 3{\cdot}2$ the clearance is positive, with $b(L)$ falling from the value $0{\cdot}75$ for $L = 0$ to zero at $L = 3{\cdot}2$. (In these cases, elastic distortion of pellet and tube is still necessary, however, where the film thickness adds to the effective thickness of the pellet.) On the other hand, the cases $L > 3{\cdot}2$ are those with negative clearance, for which film thickness produces distortion additional to what the pellet geometry would already demand.

In figure 1, the dotted curve gives the result (29) of the analysis for small $L$, which is seen to be good for $L \leqslant 1$. The broken line gives the result (54) of the analysis for large $L$. The exact values (plain line) follow this broken line closely for $L \geqslant 3$, but remain slightly above it; however, the discrepancy is decreasing fast as a proportion of the absolute value of $b(L)$.

Figure 2 shows a typical non-dimensional pressure distribution $P(X)$ for a fairly large value of $L$, namely 8. The upper curve is $P(X)$ itself, while the lower curve is the function $(-\frac{1}{2}X^2)$, so that the difference between the curves is the non-dimensional film thickness $H = P + \frac{1}{2}X^2$. If the pellet were rigid and the tube elastic, the upper curve would represent the tube shape (on a suitable scale) and the lower one the fixed pellet shape. If the pellet is elastic, however, it will participate in the distortion, but we can still say that the pressure varies as given by the upper curve and the film thickness as given by the distance between the curves.

Even for an only moderately large value $L = 8$, the layer structure predicted in §5 is clearly visible, as markings on the figure indicate. The film thickness exhibits only very gradual growth with $X$ in the central region. The boundary

layer separating this from the left-hand region of approximately constant pressure is thin, but there is a more extensive, and indeed double, boundary layer separating the central region from the right-hand region.

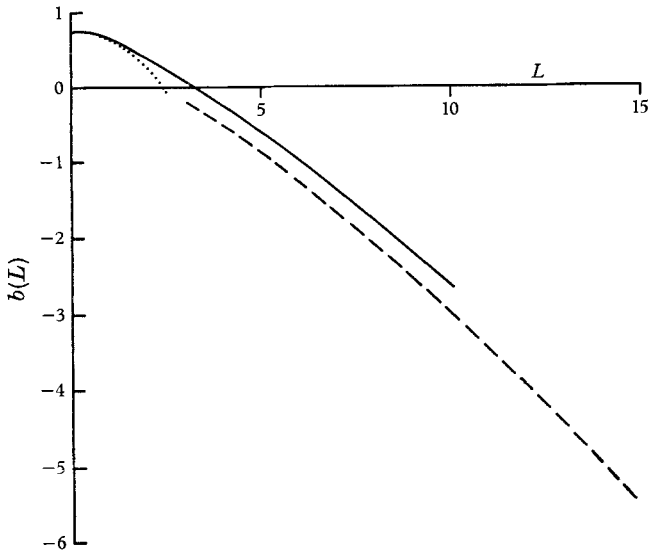


FIGURE 1. Plots, as a function of the parameter $L$, the ratio, $b(L)$, of the pellet's clearance in the tube at the downstream value of the pressure, to a typical film thickness. ·····, theory for small $L$ (§4); – – –, theory for large $L$ (§5); ——, exact values (§6).

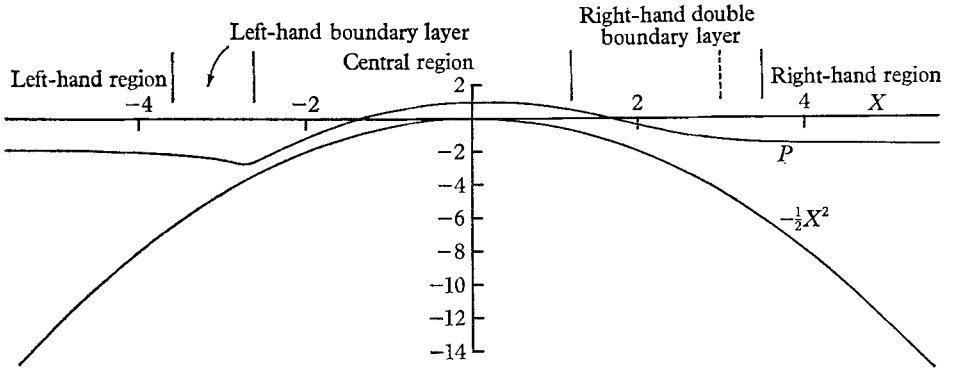


FIGURE 2. The non-dimensional pressure distribution $P(X)$ for $L = 8$, and the function $(-\frac{1}{2}X^2)$, plotted as functions of the non-dimensional axial co-ordinate $X$. The difference between the curves is the non-dimensional film thickness $H$.

A good check on the correctness of the left-hand boundary-layer analysis is given by equation (37) for $Y$, the value of $(-X)$ where $H = 1$ (so that $P$ takes its minimum value). The exact value is $Y = 2{\cdot}73$, whereas equation (37) gives $2{\cdot}83$; there is similarly close agreement for all $L \geqslant 3$.

The right-hand boundary analysis is checked in figure 3, again for the case $L = 8$, by plotting $(16L/81)^{\frac{2}{3}}(H-\frac{3}{2})$ against $(16L/81)^{\frac{1}{3}}(\frac{4}{27}L-X)$ and comparing the result with the approximate boundary-layer solution (44), that is, the

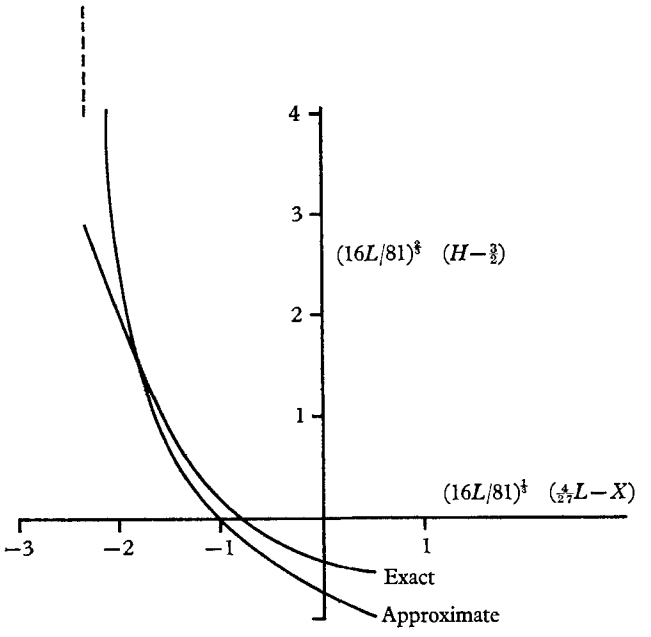


FIGURE 3. Comparison of the solution computed for $L = 8$ with the approximate boundary-layer solution (44).

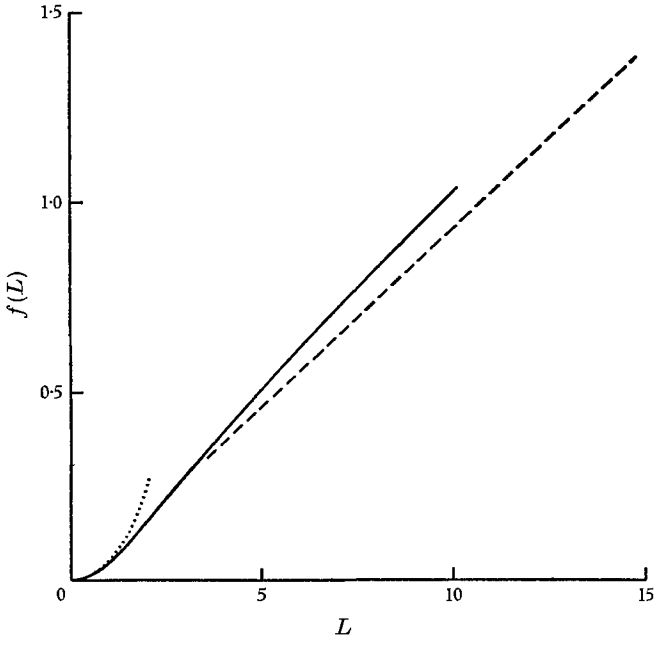


FIGURE 4. Plots as a function of the parameter $L$ the resistance integral $f(L)$, defined in equation (26). ·····, theory for small $L$ (§4); – – –, theory for large $L$ (§5); ———, exact values (§6).

logarithmic derivative of the Airy function. The agreement is again seen to be reasonably good.

Figure 4 shows the variation with $L$ in the integral $f(L)$ defined in (26). The dotted line, representing the behaviour (28) for small $L$, is close to the exact curve for $L \leqslant 1$, while for $L \geqslant 3$ the departure from the broken line, representing the simple behaviour (58) for large $L$, does not exceed 10 %. (In fact, $f(L)/L$ rises to a maximum of 0·104 at $L = 9$ and thereafter falls to its asymptotic value 0·094.) Thus, although the complicated type of approximate form (54) was needed to get relatively close to the values actually found for $b(L)$, and the simple asymptotic form (57) would have been quite inadequate, the departures of $f(L)$ from its simple asymptotic form (58) show in practice (for reasons mentioned in § 5) a much greater tendency to cancel one another out.

The fairly good agreement between the approximate theory for large $L$ and computations for all values of $L$ in the range ($L > 3{\cdot}2$) where the pellet would have negative clearance at the downstream value of the pressure tempts one to seek an expression of the asymptotic theory in simple physical terms which will make the conclusions more intelligible. This can be attempted on the following lines.

In the absence of leakback the flow relative to the pellet is due to backward traction by the tube wall moving at velocity $U$. This generates (if leakback is prevented) a negative pressure gradient (that is, a pressure falling in the direction in which the pellet is moving). Dimensional considerations cause it to vary as $\mu U/h^2$ where $h$ is the film thickness (note that in flow at low Reynolds number pressure gradients are balanced directly by viscous forces alone, without the intervention of any inertial terms involving the density $\rho$). The addition of leakback at a rate $Q$ per unit circumferential distance adds a positive pressure gradient (one which can force a net flow $Q$ backwards against viscous resistance) which similar dimensional considerations cause to vary as $\mu Q/h^3$. The sum of these negative and positive pressure gradients varying as $h^{-2}$ and $h^{-3}$ must have a negative minimum, but be able (as $h$ becomes smaller) to take any positive value.

Behind the position of maximum cross-section the geometry calls for a region of positive pressure gradient. There is no natural limit, as we have just seen, to the value this can reach, and so, as long as the gradient of film thickness remains only gradual, the pressure gradient continues to rise. It can separate only by an increase of film thickness to the rear of the pellet so rapid that the pressure itself starts to increase, while the pressure gradient rapidly reaches its negative minimum and returns to zero, in response to the rapid increase in $h$. This gives the necking at the rear, which figure 2 shows so clearly, and which might almost be confused with peristaltic propulsion of the pellet.

By contrast, at the front there is a natural limit to the region of adherence of tube wall and pellet, because the pressure gradient, negative in this region, cannot decrease beyond its permissible minimum. It can be expected, rather, to approach this minimum gradually, and remain near it in a relatively extended region, which does not involve any abrupt rise in film thickness. The film thickness increases only slowly in fact; but ultimately this permits the pressure gradient to fall to negligibly small values. The necking at the rear is not mirrored,

then, by any similar phenomenon in front, where there is rather a very smooth and gradual variation of tube radius.

It is interesting to note that the general impression given by the above physical description is still found to be valid for quite a small value of $L$, namely 1, corresponding to a substantial positive clearance of the pellet within the tube at the downstream value of the pressure. Figure 5 plots $P$ and $(-\frac{1}{2}X^2)$ for $L = 1$, just as figure 2 did for $L = 8$. The necking at the rear and smooth variation in front are not so pronounced but are still clearly visible.

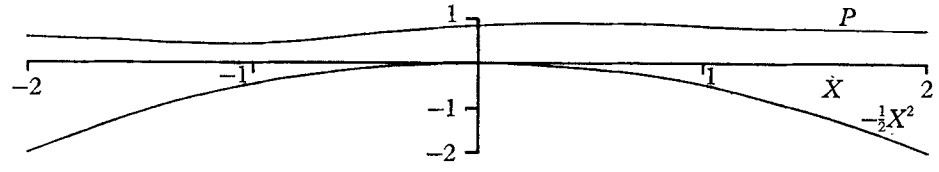


FIGURE 5. The non-dimensional pressure distribution $P(X)$ for $L = 1$, and the function $(-\frac{1}{2}X^2)$, plotted as functions of the non-dimensional axial co-ordinate $X$. The difference between the curves is the non-dimensional film thickness $H$.

It must be recognized, of course, that figures 2 and 5 show pressure distributions solely in the limiting case when the difference, pressure behind minus pressure ahead of pellet, is negligibly small compared with the variations of pressure in between. In many practical cases to which the theory could be applied (see § 7) the difference would indeed be so small as to be undetectable on the scale of such figures. In the remaining cases, however, a more realistic pressure distribution would be one in which the point of 'necking' was moved slightly forwards, and the level of pressure from that point backwards was very slightly raised above the values shown in the present diagrams.

## 7. The principal parameters of the motion and their interdependence

The results of the analysis of §§ 3–6 cannot be used directly to infer characteristics of the motion produced when tube and pellet have given geometry, elastic properties and relative velocity, and the fluid has given viscosity. This is because the necessary non-dimensionalizing of the equations had the effect that all quantities were deduced as functions of the non-dimensional parameter $L$, defined by (17). On the other hand, the value of this parameter can by no means be regarded as given, since it depends rather sensitively on the value of the typical film thickness $2Q/U$, which is one of the quantities which we particularly wish to determine.

It follows that, after computing the dependence of various physical parameters on $L$, we must proceed by elimination of $L$ to deduce the dependence of those parameters on one another. In this section, we introduce several non-dimensional parameters relevant to the motion and carry out this process of elimination of $L$ to determine their interdependence. These are new parameters, additional to the parameter $C$ defined in equation (18) as the ratio of typical film thickness to tube radius.

First we introduce a parameter

$$A = \mu U(\alpha+\beta)/r_0^2(\kappa r_0)^{\frac{1}{2}}, \tag{59}$$

which measures pellet velocity on a scale depending only on the fluid viscosity and on the geometry and elastic properties of tube and pellet, and a clearance parameter

$$B = (\alpha+\beta)[p(\infty)-p_0]/r_0, \tag{60}$$

which is the ratio of the clearance (positive or negative), that the pellet would have in the tube at the downstream value of the pressure, to the tube radius. Next, it is necessary to relate the value of a velocity parameter such as (59) to some non-dimensional form of the pressure difference. Two alternative forms will be used; the first is

$$D = [p(-\infty)-p(\infty)]r_0(\kappa r_0)^{\frac{1}{2}}/\mu U, \tag{61}$$

which we shall see relates it to the pressure difference in a stretch of purely fluid-filled tube with mean velocity and length comparable to those of the pellet; the second is

$$E = (\alpha+\beta)[p(-\infty)-p(\infty)]/r_0, \tag{62}$$

which measures it on the same scale as (60), and is the (possibly very small) difference between the clearances that the pellet would have in the tube at the upstream and downstream pressures, divided by the reference radius $r_0$.

In order that the approximate equations derived in §2 shall be reasonably accurate, we shall confine ourselves to solutions for which the parameters $B$ and $C$ are of order $10^{-1}$ or less. In order that the approximate replacement of condition (19) by equation (27) be reasonably accurate, we need also that $E$ be at least an order of magnitude smaller; that is, of order $10^{-2}$ or less. By excluding solutions for which the resistance to the pellet's motion is so great that the pressure difference required expands the gap between the tube and pellet by significantly more than 1 %, we are probably not excluding from consideration situations of great practical interest.

In terms of the parameters $L$ and $C$ which were taken as fundamental in §§3–6, the new parameters $A$, $B$, $D$ and $E$ are specified, according to equations (15), (17), (18) and (27), together with the definition of $b(L)$ as the value of $P(\infty)$ for the solution considered, as

$$A = \tfrac{1}{6}LC^{\frac{5}{2}}, \quad B = b(L)C, \quad D = 6C^{-\frac{1}{2}}f(L), \quad E = LC^2f(L). \tag{63}$$

From these relationships, with the determinations of $b(L)$ and $f(L)$ in §§4–6, it is possible to eliminate $L$ and express any three of the physically significant parameters $A$, $B$, $C$, $D$ and $E$ in terms of the other two.

For example, figure 6 shows curves of constant $A$ and curves of constant $C$ on a plot in which the abscissa is $B$ on a linear scale and the ordinate is $E$ on a logarithmic scale. This was obtained by taking in pairs particular values of $A$ and $C$ (and not only those actually shown on figure 6), deducing $L$ from the first of equations (63) and so inferring the values of $B$ and $E$. The conditions that $B$ and $C$ should be of order $10^{-1}$ or less and $E$ of order $10^{-2}$ or less were applied in selecting the curves actually plotted. Evidently $10^{-2\cdot5}$ is about the largest value of the velocity parameter $A$ for which these conditions are satisfied.

The right-hand half ($B > 0$) of the diagram corresponds to pellets with positive clearance at the downstream value of the pressure. Film thicknesses are correspondingly high and, for given velocity parameter $A$, predicted resistances are, relatively speaking, very low indeed.

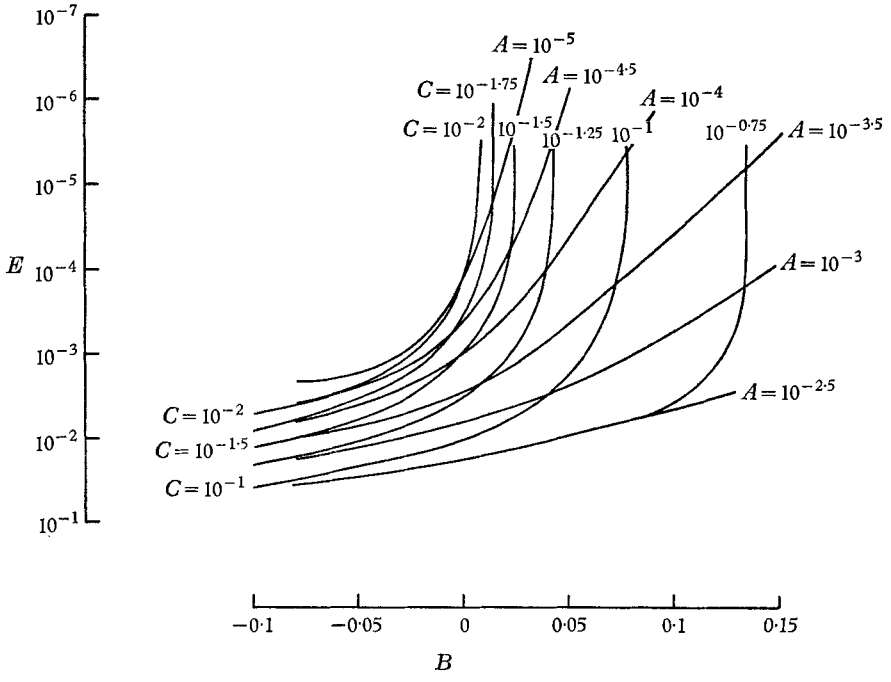


FIGURE 6. Curves of constant velocity parameter $A$ and film-thickness parameter $C$ on a plot in which the abscissa is the clearance parameter $B$ and the ordinate is the resistance parameter $E$.

The more interesting left-hand half ($B < 0$) corresponds to pellets with negative clearance at the upstream value of the pressure. Film thicknesses are considerably reduced, and become especially small for low values of the velocity parameter $A$. For higher values, $10^{-2.5}$ or more, the values of the resistance parameter $E$ may approach such an embarrassingly high level as 0·03.

The physical significance of $A$ indicates, on the other hand, that such high values will be quite exceptional in practical circumstances. If we take $2\sqrt{(r_0/\kappa)}$ as an order-of-magnitude length for the pellet (a formula chosen as being exact in the particular case when its shape is spheroidal) then the pressure drop in simple Poiseuille flow of fluid along that length of tube, of radius $r_0$, is

$$\frac{8\mu U}{r_0^2}\,2\left(\frac{r_0}{\kappa}\right)^{\frac{1}{2}} = \frac{16\mu U}{r_0^2(\kappa r_0)^{\frac{1}{2}}}. \tag{64}$$

The definition (59) means therefore that $16A$ represents the fraction of the tube radius by which the clearance between tube and pellet would change under this modest pressure drop. Accordingly, a value of $A$ as large as $10^{-2.5}$ means that the velocity $U$ is so great, and either the tube or the pellet is so compliant, that the

simple Poiseuille pressure change in fluid flow at mean velocity $U$ through the tube (without any pellets in it) would already, in a distance equal to a pellet length, change the clearance by $0{\cdot}05r_0$.

At the other end of the scale of values of $A$, a fairly large area of the diagram in the region where $B$ is negative and $A < 10^{-5}$ has been left vacant, partly to avoid overcrowding and partly because, although this area is not without its importance, the relationships between the parameters become very regular, as the curves tend to show. The most interesting feature is the progressive reduction in film thickness to very low values as $A$ decreases, and this dependence between $A$ and $C$ is shown separately on the left-hand side of figure 7 for two negative

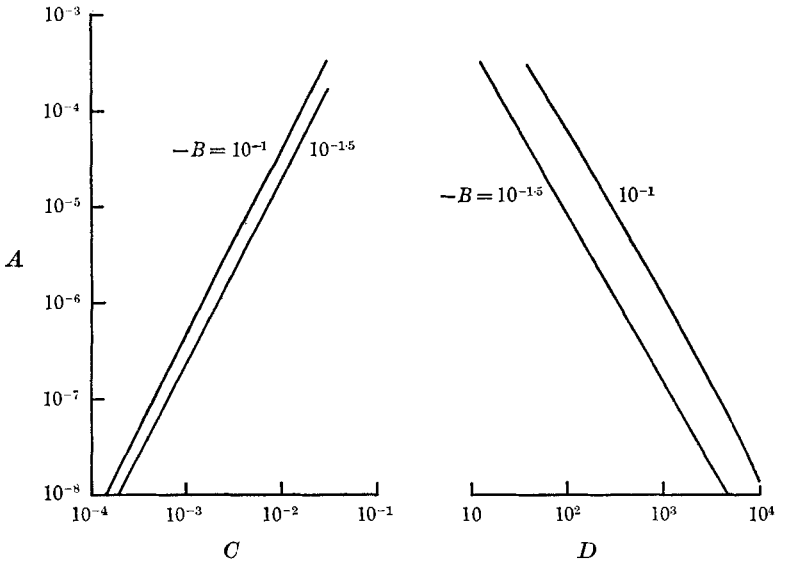


FIGURE 7. Variation of film-thickness parameter $C$ and resistance parameter $D$ with the velocity parameter $A$ for two fixed negative values of the clearance parameter $B$.

values of $B$, $-10^{-1}$ and $-10^{-1{\cdot}5}$. Exceedingly low values of $C$, less than $10^{-2}$, such as are found for values of the velocity parameter $A$ less than about $10^{-4{\cdot}5}$, mean that hydrodynamic lubrication, in requiring film thicknesses less than a hundredth of the tube radius, may for more than one reason, discussed below, cease to be possible. In the meantime we may note that it is just the conditions described in figure 7 for which the parameter $L$ takes large values (in fact, between 6 and 250).

The alternative measure of resistance given by the parameter $D$ relates the difference of pressure downstream and upstream of the pellet to the value (64) characteristic of flow at the same mean velocity $U$ in the absence of pellets. We see that values of $D$ large compared with 16 imply resistances much in excess of what a length of tube equal to the pellet length would have in the absence of the pellet.

Figure 8 plots $D$ as a function of the clearance parameter $B$ for six different values of the velocity parameter $A$. It is interesting that for positive clearances

the resistance parameter is very low indeed (*much* smaller than 16). This is because of the very effective cancelling, in the 'small $L$' regime, between regions of positive pressure gradient where the film thickness is less than $2Q/U$ and regions of negative gradient where it exceeds $2Q/U$ (see §§2–4). In this region, resistance, such as it is, increases steadily with increasing velocity.

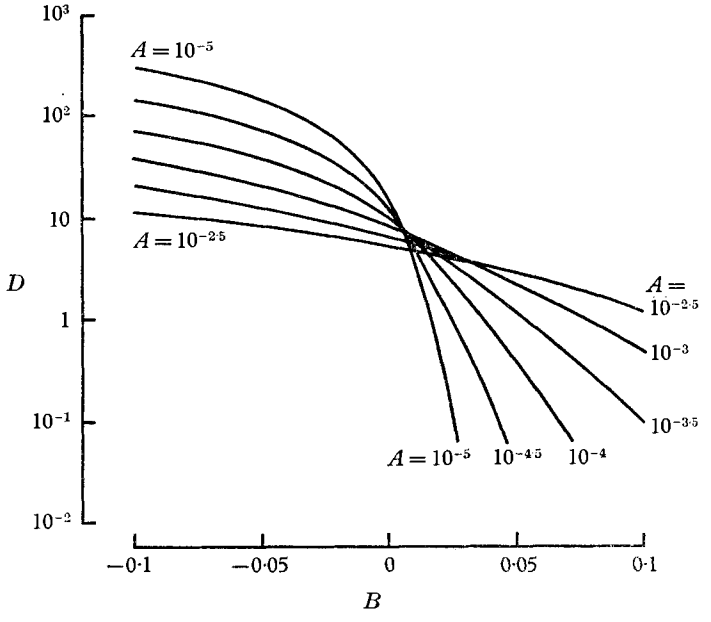


FIGURE 8. Resistance parameter $D$ plotted as a function of clearance parameter $B$ for a range of different values of the velocity parameter $A$.

The position changes completely, however, for negative values of the clearance parameter $B$. The resistance parameter $D$ now increases as the velocity parameter $A$ *decreases*. For the lower values of $A$, furthermore, $D$ is very considerably in excess of $16 = 10^{1\cdot2}$. This means that resistance is increased very many times by the fact that very thin films are generated under these circumstances.

As with figure 6, the results for very low values of $A$ are omitted from figure 8 for clarity's sake, being given rather a different form on the right-hand side of figure 7. They show that, for a given negative value of the clearance parameter $B$, the resistance parameter $D$ varies as something between $A^{-0\cdot5}$ and $A^{-0\cdot6}$. If $D$ were independent of $A$, then pressure difference would be proportional to velocity, but its actual dependence means that the pressure difference required to force the pellet at velocity $U$ varies as something between $U^{0\cdot4}$ and $U^{0\cdot5}$, falling off much slower than might have been expected at the lower velocities.

A physical interpretation of the results in figure 7 is that, as the film thickness $h$ decreases, the pressure gradients to be sustained come to depend more and more exclusively on the geometry and elastic properties of the tube and the pellet. For given velocity $U$, those pressure gradients need to be balanced by hydrodynamic terms of order $\mu U/h^2$, indicating that film thickness $h$ should vary as

$\sqrt{U}$. Furthermore, the overall pressure difference, which depends on a skin-frictional resistance to the pellet's motion of order $\mu U/h$, should also vary approximately as $\sqrt{U}$.

It is notorious that hydrodynamic lubrication may break down when the film thicknesses it requires are excessively small. Reasons for this include the effect of roughness elements on the sliding surfaces and failure of exceedingly thin layers of fluid to support shear stress. In the physiological application described in § 1, there is the additional difficulty that local high pressures near the tube wall may generate a gradual loss of fluid through the wall. If this operated on a layer already thin for lubrication-theory reasons, it is possible that the rear part of the layer might thin still further and the motion 'seize up' altogether.

The velocity of flow through the capillaries is probably controlled (see § 1) mainly by the much greater net resistance of the arterioles upstream. It is possible, however, that velocities below a certain minimum value cannot be attained because of the failure of hydrodynamic lubrication and consequent 'seizing up' of the capillary motion.

## 8. Application of numerical results to motion in the capillaries

In applying the model, and the results derived from it, to motion in the capillaries, the hardest quantities for which to choose appropriate values are $\alpha$ and $\beta$.

Rand & Burton (1964) have, however, made studies of the elasticity of red cells by finding the pressure difference necessary to draw them into micropipettes of various diameters. Their studies led them to view the red cell as a balloon with skin stretched to a tension of 0·02 dynes/cm (that is, in SI units, 0·02 mN/m). Fung (1966) supports the concept of a fluid-filled stretched membrane, and emphasizes the many modes of deformation available to a biconcave cell of this character as compression at one position is balanced against expansion at another.

It is possible to guess only a very rough order-of-magnitude value of a compliance from such a model. Amongst other things, to apply Hooke's law locally is certainly a very crude approximation, and can only give even order-of-magnitude accuracy in terms of the idea of approximating to the true complex nature of the compression of the pellet under the action of a *non-uniform* pressure distribution by means of an average compliance characteristic of a nearly uniform distribution.

To obtain this from the model, we remember that, where a membrane stretched to tension $T$ has $\kappa_1$ and $\kappa_2$ as principal curvatures in two directions at right angles, the pressure difference across it is $T(\kappa_1+\kappa_2)$. Now Rand & Burton (1964) measured the change in the larger principal curvature $\kappa_1$ at the rim of the pellet (and the change in the smaller one $\kappa_2$ can easily be measured from their photographs), when the red cell was deformed by a change in osmotic pressure difference across the membrane (which should act in much the same way as a change in mechanical pressure difference). For a reduction in distance between rim and centre of 0·46 $\mu$m the changes in $\kappa_1$ and $\kappa_2$ were 0·28 $\mu$m$^{-1}$ and 0·08 $\mu$m$^{-1}$ respectively.

If this deformation is taken as representative of all the many kinds of changes

of shape that may occur, and we estimate the change in pressure difference $T(\kappa_1+\kappa_2)$ required to cause it as

$$(0{\cdot}02\,\mathrm{mN/m})\,(0{\cdot}36\,\mu\mathrm{m}^{-1}) = 0{\cdot}072\,\mathrm{mb}, \tag{65}$$

where $1\,\mathrm{mb} = 100\,\mathrm{N/m^2}$, we obtain a compliance

$$\beta = \frac{0{\cdot}046\,\mu\mathrm{m}}{0{\cdot}072\,\mathrm{mb}} = 6\,\mu\mathrm{m/mb}. \tag{66}$$

Alternative methods of estimation using Rand & Burton's data give the same order of magnitude for $\beta$, and in the absence of other data this will be used in what follows.

By contrast, what has been done on the distensibility of capillary vessels indicates a value of $\alpha$ orders of magnitude smaller. Fung (1966) argued that the distensibility would be determined mainly by the elasticity of the surrounding tissue, which might have typical elastic modulus of order $10^7\,\mathrm{dynes/cm^2}$ (or, in SI units, $1\,\mathrm{MN/m^2}$). The compliance of a cylindrical hole with a radius of a few microns in such a medium would be of the order of $10^{-3}\,\mu\mathrm{m/mb}$. In the absence of other information, we may neglect the contribution of $\alpha$ in $\alpha+\beta$.

An order-of-magnitude value for the velocity parameter $A$ can then be obtained from (59), taking $\mu$ as a typical value 0·015 poise (or, in SI units, $0{\cdot}0015\,\mathrm{Ns/m^2}$) for the viscosity of plasma, and $r_0 = 3\,\mu\mathrm{m}$. The value of $\kappa r_0$ is difficult to estimate, but it seems likely (e.g. from curvature values indicated above) to be near 1, and its square root must be still nearer. Approximating the latter as 1, we obtain $A = 0{\cdot}01U$ when $U$ is measured in mm/s, so that, for a typical red-cell velocity of 0·1 mm/s, the value of $A$ is $10^{-3}$.

From figure 6, we see that, under conditions of negative clearance, $A = 10^{-3}$ corresponds to values of $C$ about 0·06 or 0·07, so that at a velocity of 0·1 mm/s the percentage leakback of plasma relative to red cells is estimated as 6 or 7 % in the narrowest capillaries, and a typical film thickness $r_0$ as about $0{\cdot}2\,\mu\mathrm{m}$. For velocities less than 0·1 mm/s, the film thickness will fall away from this value of $0{\cdot}2\,\mu\mathrm{m}$ in rough proportion (figure 7) to the square root of the velocity. From figure 8, again under conditions of negative clearance, we see that, when $A = 10^{-3}$, the resistance parameter $D$ takes values close to the typical Poiseuille-resistance value 16, while for lower velocities resistance will increase above this Poiseuille value in rough proportion to the inverse square root of the velocity. For comments on the possible significance of such decreases in film thickness and increases in resistance, see §1.

Warmest thanks are due, in conclusion, to all those who have kindly given the author help and advice during the preparation of this paper; particularly to Mrs N. A. Lighthill for programming the problem of §6, and over to Dr Colin Caro for taking great pains in the tendering of physiological advice.

## REFERENCES

Bretherton, F. P. 1961 *J. Fluid Mech.* **10**, 166.
Christopherson, D. G. & Dowson, D. 1959 *Proc. Roy. Soc.* A **251**, 550.
Dowson, D. & Higginson, G. R. 1960 *J. Mech. Engng Sci.* **2**, 188.

FORSTER, R. E. 1963 *Handbook of Physiology*, sec. 3, vol. 2, p. 961. Washington: American Physiological Society.

FUNG, Y. C. 1966 *Federation Proc.* **25**, 1761.

GABE, I. T. & ZATZ, L. 1968 *J. Fluid Mech.* (to appear).

GRUBIN, A. N. 1949 *Cent. Sci. Res. Inst. for Tech. and Mech. Engng*, Book no. 30 (D.S.I.R. Translation).

GUYTON, A. C. 1966 *Textbook of Medical Physiology*. London: W. B. Saunders.

LANDIS, E. M. & PAPPENHEIMER, J. R. 1963 Handbook of Physiology, sec. 2, vol. 2, p. 961. Washington: American Physiological Society.

MCDONALD, D. A. 1960 *Blood Flow in Arteries*. London: Edward Arnold.

PAPPENHEIMER, J. R. & KINTER, W. B. 1956 *Am. J. Physiol.* **185**, 377.

PROTHERO, J. & BURTON, A. C. 1961 *Biophys. J.* **1**, 565.

PROTHERO, J. & BURTON, A. C. 1962*a* *Biophys. J.* **2**, 199.

PROTHERO, J. & BURTON, A. C. 1962*b* *Biophys. J.* **2**, 213.

RAND, R. P. & BURTON, A. C. 1964 *Biophys. J.* **4**, 115.

ROACH, M. R. 1963 *Am. J. Cardiol.* **12**, 802.

ROACH, M. R. 1964 *Can. J. Physiol. Pharmacol.* **42**, 53.

WHITMORE, R. L. 1967 *J. App. Physiol.* **22**, 767.

ZUBAIROV, D. M., REPEIKOV, A. V. & TIMERBAEV, V. N. 1963 *Federation Proc. Transl. Suppl.* **23**, T317.